

Integrated Intensities of O–H Stretching Bands: Fundamentals and Overtones in Vapor-Phase Alcohols and Acids

Kristofer R. Lange, Nathan P. Wells, Keetra S. Plegge, and James A. Phillips*

Department of Chemistry, University of Wisconsin—Eau Claire, P.O. Box 4004,
Eau Claire, Wisconsin 54702-4004

Received: September 13, 2000; In Final Form: January 23, 2001

Integrated intensities have been measured for O–H stretching vibrational bands, including fundamentals and the first three overtones for methanol, ethanol, 1-propanol, 2-propanol, *tert*-butyl alcohol, 2,2,2-trifluoroethanol, nitric acid, and acetic acid. Fundamental band strengths are seen to increase with the electronegativity of the adjacent substituent, though directly analogous trends for overtones are less apparent. However, substituent electronegativity does parallel the proportional decrease in overtone intensity, relative to the corresponding fundamental. In addition, the intensities have been modeled using a two-parameter, linear-exponential dipole moment function. The agreement between observed and calculated intensities is fair, but the overall shapes of the fitted dipole moment functions also parallel the inductive nature of the substituent. Some tentative rationale for the observed intensity trends is offered, but definitive claims cannot be made without further investigation. The current results are finally compared to a few studies of C–H-containing compounds, and differences in the respective intensity data are discussed.

Introduction

Atmospheric chemists have recently generated much interest in the overtone bands of O–H stretching modes.^{1–12} For example, overtone bands of water clusters are thought to account for part of the discrepancy between observed and modeled absorption of light by the atmosphere,^{1,2} but they have eluded measurement in both field³ and laboratory studies.⁴ Furthermore, overtone-initiated photodissociation processes⁵ have been cited as significant sources of atmospheric radicals during low-light conditions.⁶ Since they dictate the overtone contribution to photolysis rate constants, absorption intensities are the key to assessing the significance of these processes. Recent modeling studies,⁷ as well as *ab initio*⁸ and empirical estimates⁹ of O–H overtone intensities for HNO₃, have reinforced the significance of overtone photoprocesses. However, intensities for photochemically active overtone bands of HNO₃ and HNO₄ have been reported only very recently,^{10–12} and the $6\nu_{\text{OH}}$ band strength for HNO₃ has yet to be measured.

Our interest has evolved in a more chemical direction, and is currently focused on exploring, and understanding, substituent effects on O–H vibrational band strengths. With this intention, we are currently assembling a catalog of O–H intensities that reflects as much chemical diversity as possible. A fundamental understanding of the factors governing O–H overtone intensities may be of indirect benefit to the atmospheric community, especially if important bands such as $6\nu_{\text{OH}}$ of nitric acid remain inaccessible to experiment. A key issue, from both the fundamental and atmospheric viewpoints, is the notion of a characteristic intensity for higher O–H overtones, a so-called “chemical transferability”. This has been noted in some studies of C–H overtone intensities,^{13,14} but there are often slight differences, even among structurally nonequivalent bonds in the same molecule.¹⁵ Observations such as this, and some objection to

the transferability notion, has lead us to think in terms of a “degree of transferability”, rather than a specific, all-encompassing intensity value for a given level of excitation. For example, among halogenated C–H species, fundamental intensities vary by 3 orders of magnitude, but converge with each subsequent level of excitation, reaching a *nearly* common value at $4\nu_{\text{CH}}$.¹⁴ The same general trend is apparent among the O–H overtone intensities reported below, but there are slight differences among the $3\nu_{\text{OH}}$ and $4\nu_{\text{OH}}$ bands, and several do exceed experimental uncertainties.

Our specific goals are to identify variations in O–H intensities from compound to compound, assess the degree of convergence among the band strengths with each level of excitation, and, ultimately, arrive at an understanding of how the chemical nature of the substituent affects the O–H vibrational intensities. The current focus is molecules with a single, isolated O–H bond, for which the vibrations are localized at low levels of excitation. We therefore interpret the spectra using the local mode model.¹⁶ The work reported here is the first extension of a preliminary study of the $3\nu_{\text{OH}}$ and $4\nu_{\text{OH}}$ bands in vapor-phase methanol, ethanol, and 2-propanol.⁹ We have remeasured nearly all the data published in that report, and have now measured the $2\nu_{\text{OH}}$ band strengths as well. Striving to increase the number and diversity of O–H-containing compounds, we now also report fundamental and overtone intensities for 1-propanol (a longer-chain primary alcohol), *tert*-butyl alcohol (a tertiary alcohol), 2,2,2-trifluoroethanol (a halogenated alcohol), acetic acid (a carboxylic acid), and nitric acid (a mineral acid). Below, we will show that substituent electronegativity parallels fundamental band strength, and the degree to which overtone intensities decrease in proportion to their respective fundamentals.

Experimental Section

All commercially available samples used were of the highest obtainable purity, and were used without further purification aside from being degassed via several freeze–pump–thaw

* To whom correspondence should be addressed: E-mail: phillija@uwec.edu. Phone: (715) 836-5399. Fax: (715) 836-4979.

TABLE 1: Band Centers and Spectroscopic Constants^a

	$1\nu_{\text{OH}}$	$2\nu_{\text{OH}}$	$3\nu_{\text{OH}}$	$4\nu_{\text{OH}}$	ω_e	$\omega_e x_e$
acetic acid	3581(8)	6991(30)	10246(32)		3747(19)	83.1(66)
ethanol	3665(8)	7168(15)	10489(24)	13643(56)	3836(15)	84.8(45)
2-propanol	3655(8)	7138(15)	10447(24)	13594(56)	3827(15)	86.0(45)
methanol	3681(8)	7199(15)	10541(16)	13706(28)	3853(13)	85.0(33)
nitric acid	3551(8)	6944(15)			3707 ^b	79 ^b
1-propanol	3669(8)	7168(15)	10494(24)	13641(56)	3842(15)	86.1(45)
<i>tert</i> -butyl alcohol	3644(8)	7123(15)	10414(16)	13541(28)	3818(13)	86.5(33)
trifluoroethanol	3657(8)	7148(15)	10466(16)	13620(28)	3826(13)	84.2(33)

^a All values in cm^{-1} . Experimental uncertainties are expressed in parentheses, and reflect uncertainty in the least significant digit(s) presented (e.g., 83.1(66) means $83.1 \pm 6.6 \text{ cm}^{-1}$). ^b From ref 8.

cycles. Pure HNO_3 was prepared by dripping concentrated H_2SO_4 onto solid KNO_3 under a vacuum, and collecting the product at dry ice temperature. To minimize decomposition, the sample was warmed only to fill the cells. All sample pressures were measured with a 100 Torr capacitance manometer (MKS Baratron no. 622).

Fundamental intensities were measured on a Nicolet 5DXC FTIR spectrometer at 4 cm^{-1} resolution, in an 18 cm gas cell with CaF_2 windows. The rotational structure was not resolved. Overtone intensities were measured on a newly built, scanning UV/vis/near-IR spectrometer. In this system, light from a quartz-tungsten-halogen lamp was focused onto the entrance slit of an Acton Spectra-Pro 300 monochromator (0.3 m). The exiting beam was collimated, sent through the sample cell, and focused onto a photodiode detector. For intensity measurements, the resolution was typically 3 nm, and the sampling interval was 0.5 nm. Survey scans were recorded at higher resolution (0.8 nm bandwidth, 0.1 nm sampling interval), enabling a slightly more precise determination of band centers, though this was still not sufficient for resolving rotational structure. First, overtone measurements were made in 18 or 30 cm single-pass cells, and higher overtones were measured with a commercial multipass cell (0.75–21.75 m). All were fitted with CaF_2 windows. An InGaAs photodiode (Thor Labs) was used for the first overtone measurements, and a Si photodiode was used for the higher overtones.

The path length settings of the multipass cell were checked against NO_2 absorbance cross section measurements in the 675–695 nm range.¹⁷ The agreement was fair, usually within the 5% quoted uncertainty in the NO_2 cross sections, and no systematic deviation from the manufacturer's specified path lengths was apparent. A precise comparison of the spectra was not possible, because the experimental conditions could not be matched. We also note that the current results for the $3\nu_{\text{OH}}$ band intensity differ from those in ref 9 by only +12%, –5%, and –2%, respectively, for methanol, ethanol, and 2-propanol. This suggests that any systematic path length error is no greater than other sources of random measurement error (which we address below).

Results

A sample spectrum, showing the region of the ethanol $3\nu_{\text{OH}}$ and $4\nu_{\text{OH}}$ bands is displayed in Figure 1. Two distinct features appear for the $4\nu_{\text{OH}}$ band (734 nm), arising from two distinct conformations in the room-temperature sample. Additional splittings in the $3\nu_{\text{OH}}$ band (953 nm) are due to the unresolved P-, Q-, and R-branches of each conformer. Combination bands built upon $3\nu_{\text{OH}}$, and the $4\nu_{\text{CH}}$ (~925 nm) band, are also discernible in Figure 1, but no effort was made to analyze any of these bands. Absorption frequencies for most of them have been measured previously at higher resolution.¹⁷ Band centers for the O–H stretching bands are listed in Table 1. For

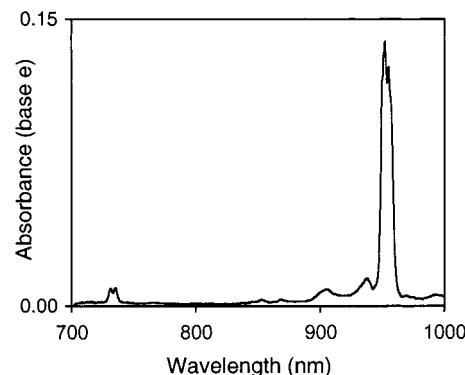


Figure 1. A sample spectrum of ethanol vapor showing the region of the second and third O–H overtone bands. The sample pressure was about 20 Torr (at 23 °C), and the path length of the multipass cell was set to 9.75 m.

molecules with a single conformer, the values reflect observed peak maxima, and the quoted uncertainty is twice the experimental resolution. The exception is a few of the fundamentals with sharp Q-branches, for which band centers were estimated by an intensity-weighted average over the width of the band.

The occurrence of two (or more) conformers complicates the interpretation of the spectra of ethanol, 2-propanol, and 1-propanol. Fang and Compton¹⁸ previously identified and assigned distinct O–H stretching bands for each stable conformer of all these species. In most instances, the bands were substantially overlapped, even at the slightly higher resolution used in that work.¹⁸ This, and the absence of reliable energy (and entropy) differences between the various conformations, makes it quite difficult to assess the integrated band strengths of specific, individual conformer species, without the risk of substantial systematic error. We note that relative overtone intensities ($\Delta\nu_{\text{OH}} = 3$) were used for an experimental determination of the enthalpy difference between *trans*- and *gauche*-ethanol, and that the analysis was based on the assumption that the strengths of the individual conformer bands were equal.¹⁹ In light of this, and the difficulties noted above, we opted to integrate over all conformer bands in the intensity analysis, and obtain a common band center for each multiplet, on the basis of an intensity-weighted average over the entire integration range. Accordingly, we assigned larger uncertainties to the band centers (see Table 1). The intensities, on the other hand, are actually population-weighted averages of all conformers present. It is worthy of note that the band shapes for the trifluoroethanol spectra indicate that only a single conformer is present at room temperature, or that the bands of all stable conformers are nearly coincident.

Band centers were fit to a Morse-like energy level expression, with a single anharmonicity constant, viz.

$$E_v = \omega_e(v + 1/2) - \omega_e x_e (v + 1/2)^2 \quad (1)$$

TABLE 2: Measured, Modeled, and Relative O–H Vibrational Band Intensities^a

		$1\nu_{\text{OH}}$	$2\nu_{\text{OH}}$	$3\nu_{\text{OH}}$	$4\nu_{\text{OH}}$
acetic acid (CH ₃ COOH)	measured	8.73(87)E–18	5.72(57)E–19	3.10(45)E–20	
	model	9.01E–18	5.01E–19	3.53E–20	3.27E–21
	$I_{01}/I_{0\nu}$ ^b	1.0	15	280	
ethanol (CH ₃ CH ₂ OH)	measured	2.73(14)E–18	3.62(17)E–19	2.24(13)E–20	1.52(19)E–21
	model	2.92E–18	2.63E–19	2.24E–20	2.31E–21
	$I_{01}/I_{0\nu}$	1.0	7.5	120	1800
2-propanol (CH ₃) ₂ CHOH)	measured	1.96(10)E–18	4.17(21)E–19	2.05(12)E–20	1.61(13)E–21
	model	2.12E–18	2.21E–19	2.00E–20	2.16E–21
	$I_{01}/I_{0\nu}$	1.0	4.7	96	1200
methanol (CH ₃ OH)	measured	3.28(16)E–18	2.71(14)E–19	2.40(15)E–20	1.69(14)E–21
	model	3.37E–18	2.57E–19	2.06E–20	2.05E–21
	$I_{01}/I_{0\nu}$	1.0	12	140	1900
nitric acid (O ₂ NOH)	measured	9.46(47)E–18	3.32(17)E–19	2.90E–20 ^c	2.80E–21 ^c
	model	9.38E–18	3.39E–19	1.93E–20	1.53E–21
	$I_{01}/I_{0\nu}$	1.0	29	330	3400
1-propanol (CH ₃ CH ₂ CH ₂ OH)	measured	2.56(13)E–18	4.38(22)E–19	2.07(13)E–20	1.39(11)E–21
	model	2.80E–18	2.26E–19	1.87E–20	1.90E–21
	$I_{01}/I_{0\nu}$	1.0	5.8	120	1800
<i>tert</i> -butyl alcohol (CH ₃) ₃ COH)	measured	1.54(08)E–18	2.25(11)E–19	2.04(17)E–20	1.69(14)E–21
	model	1.61E–18	1.95E–19	1.87E–20	2.09E–21
	$I_{01}/I_{0\nu}$	1.0	6.8	76	910
trifluoroethanol (CF ₃ CH ₂ OH)	measured	5.73(29)E–18	3.86(19)E–19	1.83(11)E–20	1.26(10)E–21
	model	6.09E–18	2.80E–19	1.81E–20	1.58E–22
	$I_{01}/I_{0\nu}$	1.0	15	310	4500

^a All values in cm/molecule. Note that “E” reflects shorthand for scientific notation, and experimental uncertainties are expressed in parentheses, and reflect uncertainty in the least significant digit(s) presented (e.g., 1.96(10)E–18 means $1.96 \times 10^{-18} \pm 0.10 \times 10^{-18}$ cm/molecule). ^b $I_{0\nu}/I_{01}$ is the intensity ratio obtained by dividing the overtone band strength by that of the fundamental. ^c Values from ref 11. Others are given in refs 8 and 10. We chose these only because they were the most recent.

Constants obtained from the fits are also displayed in Table 1. The quoted uncertainties encompass the prior determinations,¹⁸ in which each conformer was analyzed independently. Our data do reflect the previously noted trends in the spectroscopic constants,¹⁸ despite the slightly lower resolution used here. Specifically, the anharmonicity constants of the alcohols are identical within experimental error, but the frequencies tend to decrease with the size of the organic substituent. The trifluoroethanol constants fit this trend as well, though ω_e is slightly smaller than those of the nonhalogenated, primary alcohols. Both ω_e and $\omega_e\chi_e$ for the acetic acid and nitric acid⁸ are slightly smaller, and though $\omega_e\chi_e$ for acetic acid is still within 1 standard error of the other molecules, this does suggest slight differences between the O–H potentials of the alcohols and the acid species.

Intensities were obtained via linear regression of integrated absorbance (\tilde{A} , cm^{–1}, base e) versus concentration (c , molecules/cm³), viz.

$$\tilde{A} = \tilde{\sigma}cl \quad (2)$$

Dividing the “slope” by the path length (l , cm) yields the integrated absorbance cross section ($\tilde{\sigma}$, cm/molecule). All \tilde{A} values were corrected for apparent shifts in the baseline and, occasionally, partial overlap with other bands. Aside from the acetic acid data, Beer’s law plots were quite linear, and the resulting intercepts were small, nearly always less than 5% of the lowest integrated absorbance value in the regression. Rerunning the regressions with the intercept constrained to zero generally had a very small effect on the cross section values. Changes of less than a few percent were typical. For acetic acid, Beer’s law plots in total sample concentration were very nonlinear, since it is extensively dimerized at room temperature. Linear plots were obtained with absorbance plotted against

monomer concentration calculated from the total sample pressure and the experimentally determined equilibrium constant.²⁰

Experimental intensities are listed in Table 2. We made a great effort to identify sources of error in the band strengths, and assess their magnitude. The statistical errors from the regression analyses were quite small, less than 1% for all fundamental and $3\nu_{\text{OH}}$ bands. Since smaller absorbance values were measured for the $2\nu_{\text{OH}}$ and $4\nu_{\text{OH}}$ bands, the statistical errors are somewhat larger, but still only 1–2%. We explicitly checked the resolution dependence of the intensity results by remeasuring the methanol $1\nu_{\text{OH}}$ and $3\nu_{\text{OH}}$ bands at several different experimental bandwidths. Intensities varied by less than 3% for both bands. Using the same methanol bands, we explicitly assessed the effect of pressure broadening by charging the cells with about 1 atm of total pressure with nitrogen gas following the sample fill, as in ref 13. Again, the measured intensity values changed by less than 3%.

We ultimately arrived at the following uncertainty estimates: 5% for $1\nu_{\text{OH}}$, 5% for $2\nu_{\text{OH}}$, 6% for $3\nu_{\text{OH}}$, and 8% for $4\nu_{\text{OH}}$. The basis for these choices was the percent range values associated with multiple determinations of a given vibrational band, and the assumption that the relative uncertainty for a given vibrational band is similar across the entire series of compounds studied. In many instances, the actual ranges were less, but we opted for the conservative estimate of the “nominal” value for a given band. Several of the uncertainties quoted in Table 2 are slightly larger than the values noted above. These reflect situations where the range associated with two or more determinations was significantly larger than that of the other compounds for that given band. Also, the error bars for the acetic acid data were doubled, since those results are somewhat preliminary. In the multipass cell, each $3\nu_{\text{OH}}$ and $4\nu_{\text{OH}}$ band was measured at least twice, with different path length settings.

TABLE 3: Empirical $\mu(R)$ Parameters^a

	k	R_m^b		k	R_m^b
acetic acid	0.42	2.21	nitric acid	0.17	3.75
ethanol	0.40	1.60	1-propanol	0.30	1.69
2-propanol	0.39	1.51	<i>tert</i> -butyl alcohol	0.39	1.43
methanol	0.33	1.74	trifluoroethanol	0.19	2.67

^a The dipole moment functions have units of eÅ. ^b k is a proportionality constant, and R_m is the O–H distance of maximum polarity. See the text for discussion.

Eleven separate determinations of the methanol $3\nu_{\text{OH}}$ band at six different path length settings (including resolution and pressure checks) had a mere 6% range. This suggests an upper limit of random error, including that associated with path length reproducibility. Again, the agreement between the $3\nu_{\text{OH}}$ band strengths reported here and those in ref 9, which were measured in a single-pass cell, indicates that any systematic path length error is within the uncertainty estimates quoted above.

The measured overtone intensities were modeled using an empirical, one-dimensional dipole moment function, originally due to Mecke.²¹

$$\mu(R) = kR^m \exp(-R/mR_m) \quad (3)$$

In (3), R is the O–H distance, k is a proportionality constant, and R_m is the O–H distance of maximum polarity. We chose the “linear-exponential” form ($m = 1$) of this equation, which has been used in several instances to model C–H intensities,^{14,21,22} and more recently even those of heavier group IV hydride bonds.²³ To our knowledge, this is the first application of this model to O–H bands (aside from the preliminary results reported in ref 9). We utilized analytical expressions for the dipole moment matrix elements²⁴ that require ω_e , $\omega_e\chi_e$, and R_e , the equilibrium O–H bond length, as input parameters. The latter was set to a nominal value of 0.96 Å.²⁵ The intensities ($I_{0\nu'}$) are related to the transition dipole moment integral by

$$I_{0\nu'} = \frac{8\pi^3}{3hc(4\pi\epsilon_0)} \nu_c |\langle \nu' | \mu(R) | 0 \rangle|^2 \quad (4)$$

in which ν_c is the approximate center frequency and the constants as shown are appropriate for SI units. Using (3) and (4), we fit the observed intensities of each compound to two parameters: k and R_m . Optimized values are listed in Table 3. The agreement between measurement and model is consistently good for fundamentals (0.8–8%). Agreement with overtones is highly variable, and the disagreement is occasionally as high as 50%. This is somewhat discouraging since the model values result from a best fit to the experimental data, but this level of agreement is consistent with that encountered in other studies.^{14,22,23}

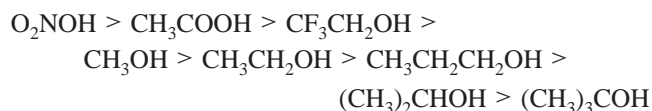
Sensitivity to the input values was assessed by explicitly changing them and rerunning the model using the methanol data. When R_e and ω_e were changed by 0.01 Å and 13 cm⁻¹ (1 standard error), the modeled intensities changed by less than 0.2%, while k and R_m changed by less than 0.5% and 2%, respectively. Not surprisingly, the effect of changing $\omega_e\chi_e$ by 1 standard error (3.3 cm⁻¹) was more significant, but the calculated intensities changed by only 2%, and the overall agreement with the experimental results was, in fact, slightly worse. The empirical parameters, k and R_m , did change significantly, by 8.7% and 2.7%, respectively. This suggests to us that the primary shortcoming regarding agreement between measurement and model is an inadequacy of the linear-exponential form of the dipole moment function. Our future

efforts will be directed toward more general forms of the dipole moment function in an attempt to improve the agreement between measured and modeled intensities.

Discussion

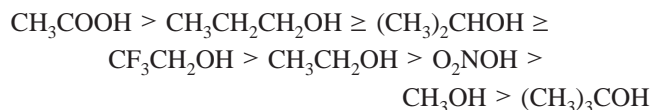
A few general trends are apparent among the experimental intensities in Table 2. As a whole, they decrease by about 1 order of magnitude with each subsequent level of excitation. The overall spread in fundamental band strengths is about a factor of 6, and the range of intensity values compresses with each level of excitation, varying by factors of 2.5, 1.9, and 1.3 for $2\nu_{\text{OH}}$, $3\nu_{\text{OH}}$, and $4\nu_{\text{OH}}$, respectively. There does seem to be some degree of transferability, starting at $3\nu_{\text{OH}}$, especially among the alcohols. However, there are observable differences that exceed experimental error, and the nitric acid $4\nu_{\text{OH}}$ value lies well outside those of the other compounds. Interestingly, the collection of results for $3\nu_{\text{OH}}$ and $4\nu_{\text{OH}}$ for HNO₃, HNO₄, and H₂O₂^{10–12} suggests that there is a significant degree of transferability within a class of inorganic O–H molecules. While these observations are at odds with any notion of an across-the-board transferability for O–H overtone intensities, the range of values obtained thus far certainly does compress with each level of excitation, at least up to $4\nu_{\text{OH}}$.

There are also notable trends among the compound-to-compound variations in the intensity values, and often they do parallel the electronegativity of the substituent bonded to the O–H unit. For fundamentals, the pattern is quite clear: stronger bands are observed for molecules with more electron-withdrawing substituents, and vice versa, viz.



For the primary alcohols, the trend toward decreasing intensity is apparent as the length of the carbon chain increases. Also, the bands get weaker as carbon adjacent to the O–H is varied from primary to tertiary. Interestingly, the empirical R_m values in Table 3 also parallel the fundamental band strengths, with the exception of acetic acid.

Analogous trends are much less apparent among overtones. In particular, the $2\nu_{\text{OH}}$ values show no correlation whatsoever with substituent electronegativity, as they rank in the following order:



To a lesser extent, the $3\nu_{\text{OH}}$ and $4\nu_{\text{OH}}$ band strengths do seem to parallel inductive character, like the $1\nu_{\text{OH}}$ values, but the differences are slight, and sometimes do not exceed experimental error. Furthermore, the trifluoroethanol data clearly oppose this trend, as the $3\nu_{\text{OH}}$ and $4\nu_{\text{OH}}$ values are the lowest listed, while those of HNO₃, HNO₄, and H₂O₂ are significantly higher.^{10–12}

While no clear correlation between substituent electronegativity and the *absolute* values of the overtone intensities is evident, a clear pattern emerges upon an examination of overtone intensity *ratios*, relative to their corresponding fundamentals. These relative intensity values ($I_{01}/I_{0\nu'}$) are also listed in Table 2, and they convey the degree of “falloff” in the band strengths with each subsequent level of excitation. It is apparent that the proportional decrease in intensity, relative to the fundamentals, is greater for the molecules with the more electron-withdrawing

substituents, and vice versa. The degree of falloff between successive overtone bands (e.g., I_{02}/I_{03}) varies much less, and the overall variation decreases with successive excitation, so those values are not listed. In any event, the peculiar ordering of the $2\nu_{\text{OH}}$ intensity values can be rationalized, at least on a phenomenological basis, as follows. The O–H fundamental is brightest for compounds with electron-withdrawing substituents, but there is a correspondingly high degree of falloff from $1\nu_{\text{OH}}$ to $2\nu_{\text{OH}}$ (a factor of 29 for nitric acid). With electron-releasing substituents, the fundamental is less intense, but the falloff is also less severe (a mere factor of 4.7 for 2-propanol).

The underlying nature of these trends remains somewhat puzzling, though they presumably arise from systematic effects in the potential energy curve, and/or the dipole moment function. With regard to the former, we note that overtone intensities are quite sensitive to the inner potential wall,^{26,27} and that the main contribution to overtone intensity is due to mechanical anharmonicity.²⁷ In fact, C–H overtone intensities have been modeled with a linear dipole function and constant relating to the inner potential wall.²⁶ Our frequency data, and those recorded previously,¹⁸ indicate that the O–H potentials of these species are about equally anharmonic, but there is a trend toward lower ω_e values as the substituent becomes more electron-releasing. However, the fact that ab initio predictions of overtone intensities require long expansions of the dipole function (seventh order in ref 8) implies a significant sensitivity to the dipole function, well beyond the linear term. Moreover, even (purely) mechanical contributions to the intensity scale with the dipole moment derivative, which could, in principle, vary significantly from compound to compound. However, we certainly cannot rule out the possibility that at least some portion of the trends identified above stem from subtle systematic effects in the potential energy curves.

Trends among the fitted dipole moment functions clearly do parallel changes in the substituent. In turn, this may suggest that systematic variations in the dipole moment functions play a significant role in the noted intensity trends. At this point, however, we must regard this rationale as speculation, since the modeling approach clearly has some shortcomings. Most significantly, it only marginally reproduces measurements. One-dimensional functions such as this are often interpreted as H–X “bond dipole” functions,²⁴ which is a distinction we avoid. Presumably, our empirically determined functions reflect some overall shift in molecular charge distribution, though this may occur predominantly within the O–H bond. By contrast, the dipole moment function is usually represented by a three-dimensional Taylor series expansion in ab initio predictions of overtone intensities.^{9,15} From an experimental standpoint, it is impossible to separate the individual x , y , and z contributions to the measured intensities, so any empirical dipole moment function need only be one-dimensional. We finally note that our intensity data for ethanol, 2-propanol, and 1-propanol were averaged over at least two conformations, and dipole functions must reflect this averaging.

A visual inspection of the fitted dipole moment functions conveys the qualitative trends among them. A few are displayed in Figure 2, and have been set to zero at 0.7 Å for the sake of visual comparison. This is reasonable since the intensity measurements probe only the function’s shape in the region of R_e , not its actual value. We noted above that the R_m values increased with fundamental band strength and, in turn, with the substituent electronegativity. Beyond this, the plots in Figure 2 show that the functions become both steeper and less curved as substituent electronegativity increases. Presumably, the

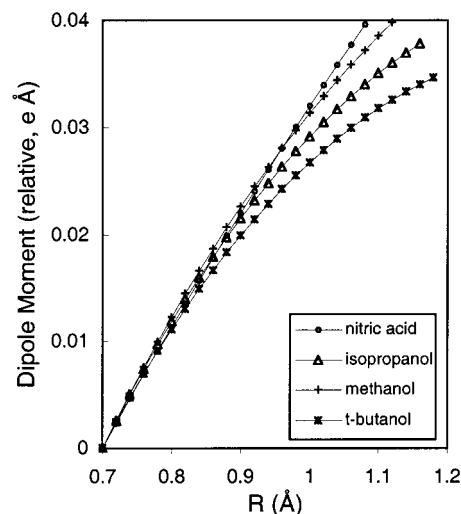


Figure 2. Selected dipole moment functions obtained from least-squares fits to measured intensities. See the text for discussion.

observed “steepness” may reflect the dipole moment derivative in a Taylor series representation, and in turn, this would account for the trend in fundamental band strengths. Perhaps the “curvature” reflects higher-order derivatives in a Taylor series representation, or electrical anharmonicity. If so, it could account for the observation that compounds with more electron-releasing substituents, and more highly curved $\mu(R)$ plots, exhibit less intensity falloff. At this point, however, we refrain from making any definitive claims with regard to the “true” dipole moment functions until they have been probed computationally, or we develop an empirical function that more closely reproduces the experimental data.

Previously measured C–H vibrational intensities that have been modeled with the linear-exponential function provide an interesting set of data for comparison. The overall intensity trend among halogenated C–H compounds¹⁴ mimics that described above, but it is much more extreme. Fundamental band strengths vary by a factor of 3000, but by $4\nu_{\text{CH}}$, the intensities converge to within a factor of 2.5. The overall range of R_m values among seven compounds varied from 1.05 to ~ 6.0 Å.¹⁴ Among nonhalogenated C–H species,²⁴ a much smaller range is noted, and R_m values are generally less than R_e (0.43–0.88 Å), suggesting a decrease in polarity as the bond is stretched. For both C–H and O–H molecules, the degree to which the intensities vary from compound to compound is paralleled by a corresponding variation in the parameter(s) of the empirical dipole function (R_m in this case). These observations support the notion that variability in the dipole moment functions is the primary reason behind compound-to-compound variations in intensities, as well as the differences between the O–H and C–H data. A similar suggestion regarding the C–H data was made by the authors of ref 13, with some hesitation. Again, we emphasize that further investigation is warranted before more definitive claims can be made. However, the notion of a more variable dipole moment function for C–H bonds is chemically justifiable, in that an O–H bond is much less polarizable than a C–H bond. Clearly, O–H bonds are always polar, and while C–H bonds are typically nonpolar, they can become polar in the presence of electronegative substituents. Thus, the suggestion that the differences observed between O–H and C–H vibrational intensities are due to variations in the respective dipole moment functions is in accord with simple chemical intuition.

Conclusion

We have measured integrated absorbance cross sections for several O–H stretching bands, including fundamentals and first three overtones for six alcohols and two acids, all in the vapor phase. We have very carefully evaluated the experimental results and expended much effort identifying and assessing sources of error in these data. The fundamental intensities were found to increase systematically with the electronegativity of the substituent. Furthermore, the degree of overtone intensity falloff, relative to the fundamental, was found to be more extreme for the species with electronegative substituents, and vice versa. A cursory examination of empirically determined dipole moment functions did suggest underlying reasons for these trends, but this cannot be considered definitive, because of the model's simplicity, and its marginal agreement with the measurements. Future efforts will be concerned with expanding the number and diversity of compounds in our O–H intensity catalog, and increasing the sophistication and flexibility of our modeling approach.

Acknowledgment. Acknowledgment for financial support of this work is made to the donors of the Petroleum Research Fund, administered by the American Chemical Society. This work was also supported by an award from Research Corp. The University of Wisconsin—Eau Claire provided additional financial support and facilities. N.P.W. acknowledges a Jean Dreyfus Boissevain Undergraduate Scholarship for Excellence in Chemistry, sponsored by the Camille and Henry Dreyfus Foundation. J.A.P. acknowledges a prior collaboration with J. Orlando, G. Tyndall, and V. Vaida, as well as insightful suggestions from D. J. Donaldson, all of which helped initiate and motivate this project.

References and Notes

(1) (a) Goss, L. M. Ph.D. Thesis, University of Colorado, 1998. (b) Chylek, P.; Fu, Q.; Tso, H. C.; Geldart, D. J. W. *Tellus A* **1999**, *51*, 304.

- (2) Low, G. R.; Kjaergaard, H. G. *J. Chem. Phys.* **1999**, *110*, 9104.
 (3) Daniel, J. S.; Solomon, S.; Sanders, R. W.; Portmann, R. W.; Miller, D. C. *J. Geophys. Res.*, *D* **1999**, *104*, 16785.
 (4) Goss, L. M.; Sharp, S. W.; Blake, T. A.; Vaida, V.; Brault, J. W. *J. Phys. Chem. A* **1999**, *105*, 8620.
 (5) See, for example: Sinha, A.; Vander Wal, R. L.; Crim, F. *J. Chem. Phys.* **1990**, *92*, 401.
 (6) Donaldson, D. J.; Frost, G. J.; Rosenlof, K. H.; Tuck, A. F.; Vaida, V. *Geophys. Res. Lett.* **1997**, *24*, 2651.
 (7) Donaldson, D. J.; Tuck, A. F.; Vaida, V. *Phys. Chem. Earth, C* **2000**, *25*, 223.
 (8) Donaldson, D. J.; Orlando, J. J.; Amann, S.; Tyndall, G. S.; Proos, R. J.; Henry, B. R.; Vaida, V. *J. Phys. Chem. A* **1998**, *102*, 5171.
 (9) Phillips J. A.; Orlando, J. J.; Tyndall, G. S.; Vaida, V. *Chem Phys. Lett.* **1998**, *296*, 377.
 (10) Brown, S. S.; Wilson, R. W.; Ravishankara, A. R. *J. Phys. Chem. A* **2000**, *104*, 4976.
 (11) Zhang, H.; Roehl, C.; Sander, S. P.; Wennberg, P. O. *J. Geophys. Res.*, *D* **2000**, *105*, 14593.
 (12) Fono, L.; Donaldson, D. J.; Proos, R. J.; Henry, B. R. *Chem. Phys. Lett.* **1999**, *311*, 131.
 (13) Burberry, M. S.; Albrecht, A. C. *J. Chem. Phys.* **1979**, *71*, 4768.
 (14) (a) Amrein, A.; Dübal, H.-R.; Lewerenz, M.; Quack, M. *Chem. Phys. Lett.* **1984**, *112*, 387. (b) Lewerenz, M.; Quack, M. *Chem. Phys. Lett.* **1986**, *123*, 197.
 (15) Kjaergaard, H. G.; Turnbull, D. M.; Henry, B. R. *J. Phys. Chem. A* **1997**, *101*, 2589.
 (16) Henry, B. R. *Acc. Chem. Res.* **1977**, *10*, 207.
 (17) Schnieder, W.; Moortgat, G. K.; Tyndall, G. S.; Burrows, J. P. *J. Photochem. Photobiol., A* **1987**, *40*, 195.
 (18) Fang, H. L.; Compton, D. A. C. *J. Phys. Chem.* **1988**, *92*, 6518.
 (19) Fang, H. L.; Swofford, R. L. *Chem. Phys. Lett.* **1984**, *105*, 5.
 (20) Clague, A. D. H.; Bernstein, H. J. *Spectrochim. Acta, A* **1969**, *25*, 593.
 (21) Mecke, R. Z. *Elektrochem.* **1950**, *54*, 38 and references therein.
 (22) Longhi, G.; Zerbi, G.; Ricard, L.; Abbate, S. *J. Chem. Phys.* **1988**, *88*, 6733.
 (23) (a) Lin, H.; Yuan, L.-F.; Zhu, Q.-S. *Chem. Phys. Lett.* **1999**, *308*, 137. (b) Halonen, M.; Halonen, L.; Bürger, H.; Sommer, S. *J. Phys. Chem.* **1990**, *94*, 5222.
 (24) Schek, I.; Jortner, J.; Sage, M. L. *Chem. Phys. Lett.* **1979**, *64*, 209.
 (25) Huheey, J. E. *Inorganic Chemistry*, 3rd ed.; Harper & Row: New York, 1983.
 (26) Medvedev, E. S. *Chem. Phys. Lett.* **1985**, *120*, 173.
 (27) Lehmann, K. K.; Smith, A. M. *J. Chem. Phys.* **1990**, *93*, 6140.